Large-Larmor-Radius Interchange Instability

B. H. Ripin, E. A. McLean, C. K. Manka, C. Pawley,[a] J. A. Stamper, T. A. Peyser,[a] A. N. Mostovych, J. Grun, A. B. Hassam,[a] and J. Huba

Naval Research Laboratory, Washington, D.C. 20375

(Received 15 June 1987)

We observe linear and nonlinear features of a strong plasma–magnetic-field interchange Rayleigh-Taylor instability in the limit of large ion Larmor radius. The instability undergoes rapid linear growth culminating in free-streaming flute tips.

PACS numbers: 52.35.Gz, 52.35.Py, 52.50.Lp, 52.55.Lf

Plasma expanding into a magnetic field can undergo Rayleigh-Taylor or interchange instability as the heavy fluid (plasma) is decelerated by the light fluid (magnetic field).[1,2] Direct observations of this instability have been made in the limit of small ion Larmor radius (compared to density gradients and wavelengths),[3] where conventional MHD theory applies. When the ion Larmor radius becomes finite the instability is predicted to stabilize.[4] However, when the ion Larmor radius becomes large compared to other characteristic plasma dimensions, i.e., when the ions are effectively unmagnetized but the electrons are effectively magnetized, a related instability is predicted with an even higher growth rate than that of the original MHD instability.[5] The recent barium-release space experiment with the Active Magnetospheric Particle Tracer Explorer satellite, which showed substantial structure, was in such a regime.[6] A previous laser-plasma experiment in a regime of moderate-sized ion Larmor radius also measured instability growth.[7]

In this paper, we observe a robust interchangelike instability in the limit of very large ion Larmor radius. The instability exhibits a rapid linear phase with subsequent nonlinear free-streaming flutes and examples of density clumping, flute-tip bifurcation, and interesting late-time spirallike structures.

Our experiment is comprised of an energetic laser-produced plasma expanding radially outward into a uniform magnetic field B formed by a pair of Helmholtz coils,[8] as depicted in Fig. 1. Steady-state (on the time scale of the experiment) vacuum B fields from 0 to 1 T are used. Plasma bursts are created by our focusing a beam of the Pharos III neodymium laser onto small Al (2 μm thick, 1 mm diam) disk targets. Unless noted otherwise, the nominal laser pulse has an irradiance of about 10^{13} W/cm^2, 30 J of energy, and 3-ns duration (FWHM). The principal diagnostic used to measure the plasma and instability development is a Grant Applied Physics fast-gated microchannel-plate optical camera focused onto the target midplane antiparallel (usually) to the magnetic field lines. Shutter speeds of 1 or 2 ns are used. In addition to the gated camera, we also used ion time-of-flight detectors to measure the plasma ion velocity distribution, several small (230 μm diam, two turn) magnetic induction probes to obtain magnetic field dynamics, small Langmuir and capacitive probes to measure density gradients and fluctuations, open-shutter photography and witness plates to see persistent structure, and fiber-optic spectroscopy to estimate density profiles during the plasma/magnetic field interaction.

The velocity distribution of the expanding plasma, measured for $B=0$ with an ion time-of-flight detector, peaks at $V_0=5.4\times10^7$ cm/s with a FWHM spread of $\pm1.8\times10^7$ cm/s. The total plasma mass is about $m_0=0.2$ μg (half of which is directed into the front $\pm45°$ expansion cone), the initial electron temperature is about 500 eV, and the initial aluminum ionization state is approximately 10.[9] Thus, the ion Larmor radii are large, over 1.4 cm for 1.0 T and over 14 cm for $B=0.1$ T (on the assumption that Z is 10 or less). The electrons, on the other hand, are effectively magnetized with Larmor radii below 1 mm. Most of the experiments were performed under good vacuum (<0.1 mTorr) so that the magnetic field rather than residual collisions dominates the plasma expansion. The plasma expansion speed is very sub-Alfvénic, being more than 1 order of magnitude slower than the maximum possible Alfvén velocity in the residual background air.

In the absence of a magnetic field, the plasma expands

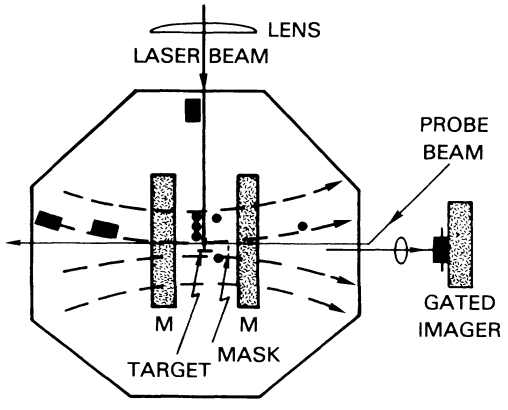

FIG. 1. Experimental arrangement for instability experiments. A schematic of the equipment is shown; ion detectors are denoted by rectangles and magnetic probes by circles.

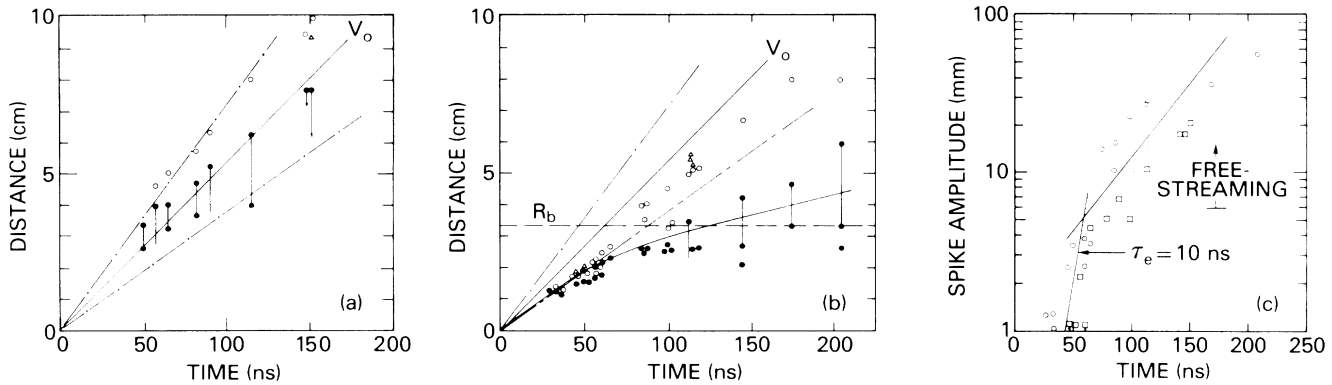

FIG. 2. Development of the instability. Locations of the instability spike tips (open circles) and main plasma boundaries (closed circles) with time for (a) the low-field (0.1 T) case and (b) the high-field (1.0 T) case. Shots denoted by triangles are plasma boundaries with zero applied magnetic field (free-streaming plasma). (c) Spike-to-bubble amplitudes vs time for 1.0 T (circles) and for 0.1 T (squares). $E_1 = 25-30$ J, $V_0 = 5.4 \times 10^7$ cm/s, and $P < 0.1$ mTorr for all cases.

radially outward from the focal region with a velocity and spread consistent with the time-of-flight ion distribution. In such expansions, most of the energy ends up in directed ion motion, with a relatively low plasma temperature (a few electronvolts).[8] When an external field is applied, the bulk plasma decelerates as it excludes magnetic field energy. Ideally, a symmetrical plasma expansion would stop near the "magnetic confinement" radius, R_b, where the excluded field energy equals the original plasma energy. For the typical 30-J shot in our experiment, R_b is 3.3 cm for $B = 1$ T and 15 cm for $B = 0.1$ T. The plasma has a deceleration of about 5×10^{14} cm/s^2 at $R = 3$ cm for $B = 1$ T [Fig. 2(b)]. The deceleration is less apparent in the 0.1-T experiments since we observe it for $R < R_b$. At intermediate magnetic field values the observed magnetic confinement distance follows the expected $B^{2/3}$ dependency within the data error bars ($\pm 20\%$). The plasma continues to cross the magnetic field beyond R_b, but at reduced speed, which is a consequence, perhaps, of our lack of a totally symmetric expansion.

The density scale lengths of the plasma fronts in a magnetic field at about 3 cm from the target fall in the range $L_n = 10 \pm 3$ mm. These estimates were obtained from the emission profiles of the time-resolved optical images, the rise times of the Langmuir and potential probe signals, and the rise time of spatially and temporally resolved Al^{+2} line (361.2 nm) emission

The array of magnetic field probes located at 1, 2, 3, 4, and 5 cm from the target show a very small (few percent at most) magnetic compression ahead of the plasma front followed by a greater than 30% diminished field within the plasma front. This field behavior is generally consistent with sub-Alfvénic plasma expansion with, perhaps, a higher than classical resistivity, e.g., $L_b \approx c/\omega_{pi}$.

Before the plasma reaches R_b, structure develops in the plasma leading (outer) edge. Distinct plasma flutes or spikes project out from the main plasma body into the magnetic field. The initial development of the instability can be seen in the low-field (0.1 T) case shown in Fig. 3(a). During the first 50 ns ($R < R_b/5$) the plasma expands with speeds near V_0 and no sign of instability is

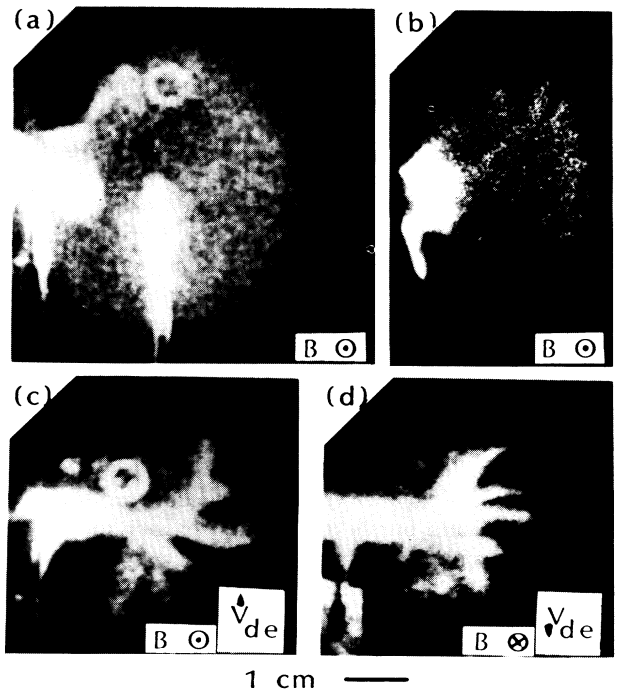

FIG. 3. Examples of the instability development. (a) 0.1-T case observed at time 115 ns. (b) Example of density clumps in the early time phase development with $B = 1.0$ T at time 59 ns. (c) Example of curved spike structure with 1.0-T field (field points out of paper) at 115 ns. (d) Same as (c) except field points into paper and $t = 100$ ns; note reversal of curvature sense. $E_1 = 25-30$ J and $P < 0.1$ mTorr for these shots.

discernible; suddenly, near $R=3$ cm, radial plasma projections appear with amplitudes comparable to their wavelengths (5–10 mm). It is clear from Fig. 2 that these plasma tips then continue to execute free streaming outward into the magnetic field. Since $R \ll R_b$, the bulk plasma is also still expanding almost uniformly. Curiously, despite a much stronger deceleration in the 1-T case ($g \propto B^2$), the instability also begins to develop at about the same distance and time as in the lower-field case. This onset behavior is consistent with the instability criterion[10] $g/L_n > \Omega_i^2/4$ which is independent of the magnetic field; Ω_i is the ion cyclotron frequency. The instability wavelengths also do not appear to be a strong function of the magnetic field strength in contrast to Ref. 7. The flute amplitude grows rapidly after onset with a linear growth rate of about 10^8 s^{-1} as seen in Fig. 2(c).[7] Unfortunately, the accuracy of the growth rate measurement (a factor of 2) is limited by the shot-to-shot reproducibility of the onset time. For comparison, the conventional (small ion Larmor radius) MHD Rayleigh-Taylor growth rate [$\gamma=(g/L_n)^{1/2}$ for $kL_n > 1$] for our parameters ($B=1$ T) is about 2×10^7 s^{-1}, whereas the large-Larmor-radius instability theory[5] predicts a 6 times faster growth rate for the observed wavelengths, which is consistent with our experimental result. At times the plasma structure initially appears as density clumps in the leading edge of the expansion plasma. This clumpinglike behavior, shown in Fig. 3(b), is a predicted characteristic of this instability.[5,10] Subsequent to the rapid linear phase of the instability the flute tips perform free streaming with speeds near V_0.

The wavelengths of the predominant flute modes (measured at the base of the flutes) are typically in the 6- to 10-mm range and are insensitive to most parameter changes. As time goes on, the instability wavelength tends to remain in this range even though the plasma continues to expand radially. Some indication of how this can occur was obtained by our placing witness plates (black Polaroid film) perpendicular to the magnetic field a few centimeters to one side of the target. These recorded time-integrated patterns of the plasma running down the field lines. Long spikes are seen in the exposures with curvature toward the midplane and additional projections formed towards the sides of the pattern with increasing distance from the source. The fact that the patterns on the witness plate are not washed out indicated that the plasma structure, once formed, does not undergo much azimuthal motion. Several examples of spike-tip bifurcation are also seen. The combination of these two effects tends to maintain constant wavelength and increase the instability mode number, $m=2\pi R/\lambda$, with distance. Sydora *et al.*[11] suggest that the azimuthal mode number of the most unstable mode would increase with decreasing charge separation between the unmagnetized ions and the plasma electrons; perhaps this is what is occurring in the experiment. It will be interesting to see if this increasing-mode-number–type behavior persists when more spherically symmetric expansions are examined.

The dominant instability wavelength, $\lambda=8\pm2$ mm, may be determined by the bulk plasma-density scale length, $L_n=10\pm3$ mm, or possibly by the magnetic diffusion length into the plasma. The collisionless skin (c/ω_{pe}) depth is only a fraction of a millimeter, but possible anomalous resistivity associated with this or another instability could push the diffusion length into the centimeter (c/ω_{pi}) range.

For some shots, the magnetic field was rotated 90° so that the instability development could be viewed perpendicular to the field lines. The plasma projections, which have the appearance of slim spikes in the end-on view, actually run smoothly along the field lines like flutes.

The free-streaming flutes exhibit some interesting features at later times. One common characteristic in the high-field experiments is the curvature and spurlike appearance of the instability fingers seen in Figs. 3(c) and 3(d). The curvature is in the electron cyclotron or electron $\mathbf{E}\times\mathbf{B}$ drift sense and reverses with magnetic field direction. It is not yet known whether the curvature arises from the spike tips moving upward or the bubble downward. But the distinct structure seen on the witness plates precludes large-scale azimuthal motion. Two possibilities are that curved flutes are caused either by $\mathbf{E}\times\mathbf{B}$-induced azimuthal electron velocity shear,[11] or as a response of large–Larmor-radius plasma to Alfvénic magnetic stresses: The theory of Hassam and Huba[5] predicts that a localized spike expanding into a magnetic field curves in the electron gyrodirection, consistent with experiment.

A number of other parameter variations were performed during the course of this investigation. The background pressure was increased up to 2 Torr of H_2 to test the effects of increasing collisionality and decreasing Alfvén speed on the instability. For the 0.1-T case viewed at 150 ns, free-streaming structure persisted up to 100-mTorr H_2 pressure at which point signatures of collisional effects were seen.[8]

In another series of shots, a 7.6-cm-diam, 3-mm-thick copper disk was placed 4 to 5 cm to one side of the target, perpendicular to the field lines, to short out the dynamic motion of the magnetic field lines. The gross feature of the instability persisted independent of whether the copper plate was grounded, ungrounded, insulated, or bare.

Finally, several shots were taken with much larger incident laser energy (400 J) but comparable irradiance at a variety of magnetic fields and pressures. The major effect of higher laser energy is to increase the plasma mass proportionally and, hence, to increase the magnetic confinement radius by $R_b \propto E_l^{1/3}$.

Another interesting observation in these experiments was the presence of a strong high-frequency (>250

MHz) signal seen in all electrical and magnetic probes whenever the Rayleigh-Taylor instability occurred. This noise is in the ion plasma or lower hybrid frequency range. The relationship of this noise to the magnetic instability is not yet clear, but may be related to the growth of very short-wavelength Rayleigh-Taylor modes, which cannot be seen in the framing pictures, or to the generation of microinstabilities in the plasma shell.[12,13]

In summary, we have experimentally demonstrated linear and nonlinear properties of a robust instability in the important regime of large ion Larmor radius and sub-Alfvénic expansion speed. The instability has many features recently predicted by a modified MHD theory[5] and computer simulation,[10] and is similar to structure in the barium-release space experiment with the Active Magnetospheric Particle Tracer Explorer satellite.[5] However, it is possible that a number of closely related instabilities, such as the lower-hybrid–drift[12,13] and Kelvin-Helmholtz[11] instabilities, may be playing a role here also.

The authors are please to acknowledge useful discussions with W. White, R. Kilb, D. Winske, and H. Dickinson. The technical assistance of J. Ford, L. Daniels, N. Nocerino, and M. Kirby is likewise appreciated. This work was supported by the Defense Nuclear Agency.

[a]Present address: Science Applications International Corp., McLean, VA 22102.

[1]M. Kruskal and M. Schwarzschild, Proc. Roy. Soc. London A **223**, 348 (1954).

[2]M. N. Rosenbluth and C. L. Longmire, Ann. Phys. (N.Y.) **1**, 120 (1957).

[3]H. Dickinson, W. H. Bostick, J. N. DiMarco, and S. Koslov, Phys. Fluids **5**, 1048 (1962).

[4]M. N. Rosenbluth, N. A. Krall, and N. Rostoker, Nucl. Fusion Suppl. Pt. 1, 143 (1967).

[5]A. B. Hassam and J. D. Huba, Geophys. Res. Lett. **14**, 60 (1987), and to be published.

[6]P. A. Bernhardt *et al.*, J. Geophys. Res. **92**, 5777 (1987).

[7]S. Okada, K. Sato, and T. Sekiguchi, Jpn. J. Appl. Phys. **20**, 157 (1981).

[8]B. H. Ripin *et al.*, in *Laser Interaction and Related Plasma Phenomena,* edited by H. Hora and G. H. Miley (Plenum, New York, 1986), Vol. 7, pp. 857–877.

[9]B. H. Ripin *et al.*, Phys. Fluids **26**, 588 (1983).

[10]J. D. Huba, J. G. Lyon, and A. B. Hassam, to be published.

[11]R. D. Sydora, J. S. Wagner, L. C. Lee, E. M. Wescott, and T. Tajima, Phys. Fluids **26**, 2986 (1983).

[12]N. A. Krall and P. C. Liewer, Phys. Rev. A **4**, 2094 (1971); D. Winske, private communication.

[13]Yu. P. Zakharov, A. M. Orishich, A. G. Ponomarenko, and V. G. Posukh, Fiz. Plasmy **12**, 1170 (1986) [Sov. J. Plasma Phys. **12**, 674 (1986)].

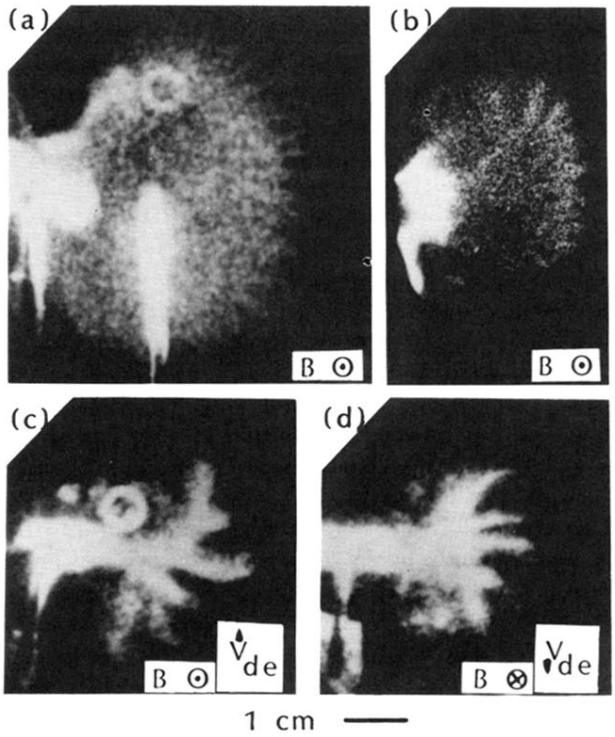

FIG. 3. Examples of the instability development. (a) 0.1-T case observed at time 115 ns. (b) Example of density clumps in the early time phase development with $B = 1.0$ T at time 59 ns. (c) Example of curved spike structure with 1.0-T field (field points out of paper) at 115 ns. (d) Same as (c) except field points into paper and $t = 100$ ns; note reversal of curvature sense. $E_1 = 25-30$ J and $P < 0.1$ mTorr for these shots.